

# Measurement of the loss tangent of a thin polymeric film using the atomic force microscope

P.M. McGuiggan<sup>a)</sup>

*Polymers Division, National Institute of Standards and Technology, Gaithersburg, Maryland 20899*

D.J. Yarusso

*3M Center, Commercial Graphics Division, St. Paul, Minnesota 55144*

(Received 16 June 2003; accepted 3 November 2003)

An atomic force microscope was used to measure the loss tangent,  $\tan \delta$ , of a pressure-sensitive adhesive transfer tape as a function of frequency (0.01 to 10 Hz). For the measurement, the sample was oscillated normal to the surface and the response of the cantilever resting on the polymer surface (as measured via the photodiode) was monitored. Both oscillation amplitude and phase were recorded as a function of frequency. The atomic force microscopy measurement gave the same frequency dependence of  $\tan \delta$  as that measured by a dynamic shear rheometer on a film 20 times thicker. The results demonstrate that the atomic force microscope technique can quantitatively measure rheological properties of soft thin polymeric films.

## I. INTRODUCTION

The mechanical<sup>1</sup> properties of thin films have become increasingly important in recent years due in large part to the development of novel coatings, magnetic storage drives, optoelectronics, and microelectromechanical systems (MEMS).<sup>1</sup> Many of these technologies consist of a coating material deposited onto a substrate of another material, and the value of the mechanical properties often reflect not only the sample of interest but also the underlying substrate. To understand and predict the performance of these systems, we must be able to measure the mechanical properties of thin films and multilayers.

Mechanical properties such as hardness, elasticity, and creep can be obtained using nanoindentation.<sup>2–7</sup> This measurement involves recording the displacement of a probe (indenter) as it indents a sample as a function of the applied force. The area of contact can be calculated from knowledge of the probe geometry or the indent can directly be imaged via microscopy. Analyses of force–distance curves and knowledge of the contact dimensions (or probe geometry) enable the mechanical properties of the film to be determined.

Atomic force microscopy (AFM) can also be used to indent thin films and obtain force–distance curves for mechanical measurements.<sup>8–11</sup> For the mechanical properties to be measured, the sample must be deformed. For this to occur, the indenter spring stiffness must be comparable to the contact stiffness. For quantitative measurements, the contact mechanics of the deformation and

the spring (cantilever) constant should be known. In general, the spring stiffness of the cantilever is difficult to measure and the contact area must be inferred, making quantitative mechanical measurements by AFM difficult.

Indentation measurements alone are generally inadequate for many polymeric samples. Polymeric materials are mostly viscoelastic (i.e., have both a viscous component as well as an elastic component).<sup>12</sup> Thus, instead of describing the polymer film in terms of a single elastic modulus value at a specific indentation depth (as obtained from nanoindentation measurements), viscoelastic materials are generally described in terms of the complex modulus, composed of a storage modulus  $G'$  and a loss modulus  $G''$ . The ratio of the loss modulus to the storage modulus is  $\tan \delta$ .

Macroscopic measurements of the viscoelastic properties of polymers generally involve dynamic testing in simple geometries.<sup>12,13</sup> Many of the dynamic mechanical tests involve alternating current (ac) modulation techniques, which give the properties of a material as a function of frequency. This allows the time-dependence of the mechanical behavior of a viscoelastic material to be measured. On the macroscopic scale, dynamic testing is well established and can include stress relaxation, creep, and sinusoidal oscillations. Often, bulk rheological measurements require films at least 0.5 mm in thickness and 4 mm in diameter.

Experimentally, the viscoelastic response of a material to dynamic tests including indentation measurements is a function of the contact conditions, such as contact geometry, penetration depth, and the loading rate. Mathematical models are required to calculate the modulus or other material property. If the sample behaves elastically,

<sup>a)</sup>Address all correspondence to this author.  
patricia.mcguiggan@nist.gov

Hertzian contact models can be used. Unfortunately, the mechanical model for viscoelastic materials is a complex problem that has only been worked out in specific limits.<sup>14</sup> For example, early work by Ting ignored adhesion.<sup>15,16</sup> Later theoretical work included adhesion, but ignored the effect of friction and adhesion hysteresis at the interface.<sup>17,18</sup> Often, the sample is considered to be infinitely thick, and the radius of the contact is assumed to be much smaller than the radius of the probe. In addition to this, most of the theoretical analyses have been done for monotonically increasing contact area as occurs during a large amplitude loading cycle.<sup>18</sup> As will be discussed later, no theoretical model exists for viscoelastic materials where the contact dimension is comparable to the film thickness and the measurement involves small amplitude oscillations, which are the conditions used in this experiment.

Although AFM measurements routinely give a qualitative map of the relative softness of a surface, obtaining a quantitative measure of the modulus of the film is more difficult. Besides indentation, quantitative measurements may involve oscillating the atomic force microscope cantilever or the surface either normal or perpendicular to the surface.<sup>19–28</sup> The measurements require knowledge of the contact radius and the normal or lateral spring constant to obtain the modulus. As previously mentioned, these can be difficult to determine accurately. In addition, only a few studies have fully measured the modulus as a function of frequency.<sup>21</sup> Often, the values obtained are different from bulk measurements, and the difference is attributed to a surface viscosity.<sup>29</sup> Significant errors in the estimation of the mechanical properties have been shown to occur for finite sample thicknesses, a poorly defined contact geometry of the pyramidal probe tip, and assumptions of linear viscoelasticity in the vicinity of the sharp, pyramidal probes generally used in AFM.<sup>30</sup>

In this paper, we describe AFM measurements of the  $\tan \delta$  of a commercial acrylic-based pressure-sensitive adhesive (PSA). By focusing on  $\tan \delta$ , we eliminate some of the unknown values necessary in the calculation of the modulus, such as contact area and spring constant. The results will be compared to bulk measurements on a film 20 times thicker. A PSA was chosen for these measurements because these adhesives exhibit viscoelastic properties, and the rheological properties of thin adhesive films are important because there is a direct connection between the rheological properties of the adhesive and adhesive performance.<sup>31,32</sup>

## II. MATERIALS AND METHODS

### A. Materials

Commercially available 3M 9485 PC (St. Paul, MN) transfer tape was used for these measurements. A transfer

tape consists of a thin film of adhesive without the polymeric backing that is commonly found on pressure-sensitive adhesive tapes. 9485 PC is an acrylic-based PSA. The sample is supplied in a roll of 25.4-mm width and 130- $\mu\text{m}$  thickness. The same roll of transfer tape was used for both AFM and bulk rheology measurements.

### B. AFM measurements

A Digital Instruments Dimension 3100 (Santa Barbara, CA) atomic force microscope was used for the measurements. A schematic diagram of the experimental design is shown in Fig. 1. In the atomic force microscope, a laser beam is reflected from the cantilever into a photodiode detector that detects shifts in the position of the reflected light. As the cantilever interacts with the substrate, the cantilever bends and the change in the deflected light is detected by the photodiode.

We modified the instrumentation of the atomic force microscope by attaching the sample to a piezo transducer (PZT). Either a Physik Instrumente P-239 PZT (Auburn, MA) linear actuator or a Piezo Systems (Cambridge, MA) low-voltage piezoelectric stack TS18-H5-202 (TS) was used for our measurements to obtain a range of amplitudes. A sine wave signal was input into the PZT via a function generator (Stanford Research Systems Model D5345, Sunnyvale, CA). The amplitudes of the PZT actuators were measured independently using a profilometer and corresponded to  $(0.579 \mu\text{m} \pm 0.03 \mu\text{m})/V_{\text{rms}}$  for the TS PZT and  $(8.28 \mu\text{m} \pm 0.12 \mu\text{m})/V$  for the P-239 PZT, where  $V$  refers to voltage and  $V_{\text{rms}}$  is the root mean square voltage. Unless otherwise noted, the  $\pm$  refers to the standard uncertainty in the measurements and is taken as one standard deviation of the observed values. Typical input voltages of the actuators were  $0.1 V_{\text{rms}}$  to  $0.3 V_{\text{rms}}$  for the TS PZT and  $0.015 V$  for the P-239 PZT. The vertical deflection photodiode signal was monitored

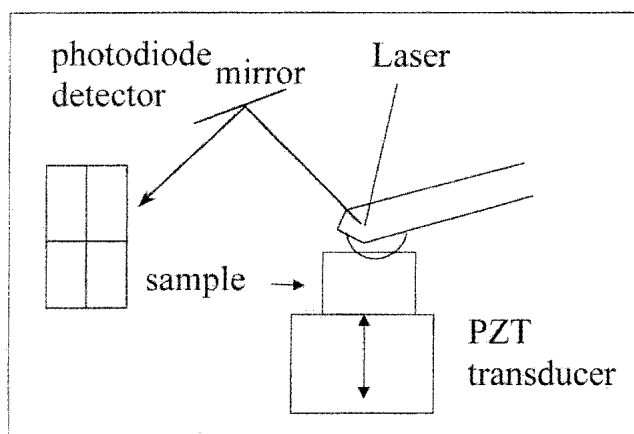


FIG. 1. Schematic diagram of the atomic force microscope. A PZT transducer oscillates the sample sinusoidally, normal to the sample surface.

(via the Signal Access Module connected between the control box and the microscope) and this signal was fed into a lock-in amplifier (Stanford Research Systems Model 830).

The phase of the photodiode output relative to the input transistor-transistor logic (TTL) signal of the function generator was measured using the lock-in amplifier. Measurements were made on a stiff surface (such as Si) prior to the measurements on the polymer sample to establish the “baseline” phase shift,  $\theta_0$ , and photodiode calibration. According to the manufacturers specifications, the PZT displacement is known to be shifted in phase from the applied voltage by a frequency-dependent angle  $\theta_0$ . Because the stiff surface can be considered to be incompressible relative to the weak atomic force microscope cantilever, the phase shift measured on Si is solely due to the PZT transducer and atomic force microscope electronics, and the amplitude of the cantilever is equal to the PZT amplitude. These assumptions ignore errors that may occur due to slip of the tip on the surface. The value of the baseline phase was independent of the amplitude but varied slightly according to the particular PZT used.

To ensure that the measurements were made in the linear regime, the harmonic response of the atomic force microscope cantilever was measured via a power spectrum analyzer. The measurements on a stiff Si surface are shown in Fig. 2. The solid circles show the 1F signal response, whereas the open and closed triangles represent the 2F and 3F harmonic response, respectively. The main contribution to the signal was at the fundamental driving frequency (1F). Second (2F) and third (3F) harmonics are

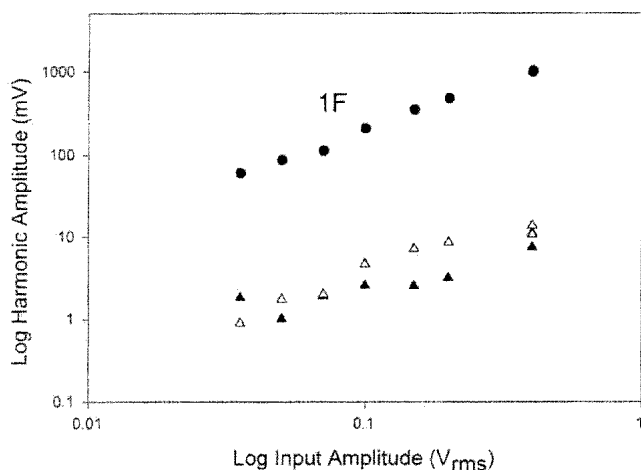


FIG. 2. Harmonic response of the atomic force microscope cantilever on a stiff silicon surface measured via a power spectrum analyzer. The solid circles, open triangles, and solid triangles represent the 1F, 2F, and 3F signal components, respectively. The input amplitude measured by profilometry as a function of input voltage is given by  $dh/dV = (0.579 \mu\text{m} \pm 0.03 \mu\text{m})/V_{rms}$ . On the stiff silicon surface, we assume that  $dh = dz$ .

measured, but these are generally less than 2% of the signal and increase linearly with amplitude, at least for the amplitudes used in this experiment. We conclude that the response is linear for the drive amplitudes used in this experiment.

The experiment was run in “contact mode.” No scanning was performed and the z-piezo feedback controls were turned off for the measurements. Commercially available microfabricated cantilever springs [DI, force modulation etched silicon probes (FESP) tapping mode] were used for the measurements. The manufacturer-listed spring constants for these cantilevers are  $50 \text{ N/m} \pm 30 \text{ N/m}$ . The experiments were run in air at  $25 \text{ }^\circ\text{C}$ , and the relative humidity was  $50\% \pm 10\%$ .

For the measurements on the polymer surface, a soda-lime glass sphere with a certified mean radius (NIST SRM 1003) was glued to the atomic force microscope cantilever using a fast-setting epoxy (Hardman epoxy).<sup>33</sup> The diameter of the sphere was  $30 \mu\text{m} \pm 10 \mu\text{m}$ . After attaching the sphere, the epoxy was allowed to dry overnight. Measurements on the adhesive sample were obtained using the glass sphere as the probe to keep the sharp atomic force microscope tip from penetrating the sample.

### C. RDA measurements

The sample was tested on a dynamic shear rheometer (Rheometrics RDA II, New Castle, DE) equipped with 25-mm-diameter parallel plates. Frequency sweeps from 0.001 Hz to 16 Hz were performed. The sample was tested at both 5% and 10% strain at the rim. At this strain, the sample remained in the linear viscoelastic regime. The sample thickness was 2.4 mm and was prepared by stacking 20 layers of the PSA. This thickness is required to give a measurable signal by RDA. The experiment was run at  $25 \text{ }^\circ\text{C}$ .

### III. THEORY

As previously mentioned, obtaining a quantitative value for the modulus of materials requires a mathematical model to interpret the data. For viscoelastic materials, mechanical models have only been worked out in specific limits, such as infinitely thick samples, a radius of contact much smaller than the radius of the probe, and loading curves where the area increases monotonically.<sup>18</sup> No theoretical model exists for viscoelastic material response under small sinusoidal oscillations, finite thickness samples, and a contact area comparable to the diameter of the probe, which are the conditions used in this experiment. Because of the lack of a rigorous model for this system and the fact that relevant experimental parameters such as area of contact and spring constants are hard to quantify, it is difficult to make a quantitative

comparison between the measurements and the elastic modulus itself. We hope that this work will spur improvements in the theory, but in the interim we will focus on a dimensionless quantity that is independent of many experimental details and also technologically important (i.e., quantification of the frequency dependence of  $\tan \delta$ ).

Consider the following experimental procedure. A probe of arbitrary geometry is brought into contact with a material and allowed to equilibrate at a fixed load. The height  $h$  of the bottom of the sample is then modulated by applying a sinusoidal voltage  $V_0(t) = V_0 e^{i\omega t}$  to a PZT. The resulting deflection of the probe produces an ac voltage  $V_1(t) = V_1 e^{i(\omega t + \theta)}$  from the photodiode signal that monitors the deflection of a laser from the probe. Because the probe is attached to a cantilever, the measured deflection will depend on both the stiffness of the sample and the stiffness of the measuring device, including the PZT and cantilever. As noted above, there is also a phase shift  $\theta_0$  between the applied voltage and the PZT displacement. Hence, the phase shift between the PZT displacement and cantilever deflection is given by  $\varphi = \theta - \theta_0$ .

We will model the experiment as a spring ( $k_{\text{AFM}}$  representing the cantilever) in series with a viscoelastic element ( $k_{\text{sample}}$  representing the polymer sample). The sinusoidal displacements of the bottom of the sample  $dh$  and cantilever  $dz$  can be written as

$$dh = c_0 V_0 e^{i(\omega t + \theta_0)} \quad , \quad (1)$$

$$dz = c_1 V_1 e^{i(\omega t + \theta)} \quad , \quad (2)$$

where  $c_0$  and  $c_1$  are real constants.

The sample will compress by an amount  $(dh - dz)$ . The force on each element (the spring and the sample) must be the same in the quasi-static limit where the acceleration of the elements is negligible. This implies

$$dz k_{\text{AFM}} = (dh - dz) k_{\text{sample}} \quad , \quad (3)$$

which can be rearranged to give the complex “spring” constant of the sample

$$k_{\text{sample}} = k_{\text{AFM}} / [dh/dz - 1] \quad . \quad (4)$$

We calibrate the instrument using a Si surface that is much stiffer than the cantilever. In this case,  $dz = dh$  and  $\theta = \theta_0$ . The ratio of the voltages gives the ratio of the unknown constants in Eqs. (1) and (2):  $V_1^0/V_0^0 = c_0/c_1$ . The ratio  $dh/dz$  is found by dividing Eq. (2) into Eq. (1) to give:

$$\frac{dh}{dz} = \frac{V_1^0}{V_0^0} \frac{V_0}{V_1} e^{-i\varphi} \quad . \quad (5)$$

The relationship between  $k_{\text{sample}}$  and the elastic modulus of the film depends on the geometry and is only known in certain limits. While none of these corresponds to our

geometry, it is useful to identify the universal aspects of the relation. Consider a sample of constant thickness  $T$  and area  $A$  between parallel plates of the same area. The force on the plates is  $A\sigma_{\perp}$ , where  $\sigma_{\perp}$  is the stress perpendicular to the plates. The displacement  $dh - dz$  is related to the corresponding strain by  $(dh - dz) = \epsilon_{\perp} T$ . Thus,  $k_{\text{sample}} = (A/T) (\sigma_{\perp}/\epsilon_{\perp})$ , where the ratio  $\sigma_{\perp}/\epsilon_{\perp}$  is independent of the magnitude of the strain for linear viscoelastic materials. To relate this ratio to a modulus, the strains along the plate  $\epsilon_{\parallel}$  must be specified. In the limit  $T \ll A^{1/2}$ , the tangential strains vanish if bonding is perfect. Then  $\sigma_{\perp}/\epsilon_{\perp} = B - 2G/3$ , where  $B$  and  $G$  are the bulk and shear moduli, respectively. Since  $B \gg G$  for polymers, measurements in this limit would provide little information about the shear modulus. In the opposite limits of  $T \gg A^{1/2}$  and zero friction, the tangential stresses vanish and  $\sigma_{\perp}/\epsilon_{\perp}$  equals Young’s modulus  $Y \equiv 3G/(1 + G/3B)$ . For typical polymers this can be approximated by  $Y \approx 3G$ , and the measurement provides direct information about the shear modulus.

Another simple limit is nonadhesive (Hertzian) contact between a rigid sphere of radius  $R$  and a flat surface of Young’s modulus  $Y$  and Poisson ratio  $\nu$ . If the surface responds elastically,  $k_{\text{sample}}$  can be obtained by differentiating the force with respect to the normal displacement. Using standard relations one finds  $k_{\text{sample}} = 2aY/(1 - \nu^2)$ , where  $a$  is the radius of the area in contact and must be small compared to  $R$  for this relation to hold.<sup>34</sup> For most polymers  $\nu \approx 1/2$ , and the sample stiffness is once more proportional to  $G$ .

Adhesive contact between a sphere and viscoelastic surface is much more complicated. The main difficulty is that there is substantial dissipation at the edge of the contact when the radius changes. The local strain rates near the edge may be quite high, causing the response to depend on the modulus at a wide range of frequencies. Theoretical studies of this problem have considered large amplitude loading and unloading curves, where the contact area changes monotonically over a wide range.<sup>18</sup> They also ignore adhesion hysteresis, which leads to a difference in adhesion energy on loading and unloading.<sup>17,18</sup> Direct observations of the contact area in macroscopic experiments show that adhesion hysteresis between dissimilar surfaces like those studied here can prevent changes in contact area over a substantial range of displacements or forces.<sup>35</sup> Thus if  $dh - dz$  is sufficiently small, changes in contact area can be ignored in our measurements. The contact mechanics problem then simplifies because a sinusoidal strain proportional to  $dh - dz$  will be applied throughout the contact region. As in the simpler geometries considered above, the value of  $k_{\text{sample}}$  would equal an appropriate length times a modulus that is proportional to  $G$  as long as the film thickness is larger than the contact diameter. Because our measurements are always in this limit, we have

$$k_{\text{sample}} = A'G = k_{\text{AFM}}/[(dh/dz) - 1] \quad (6)$$

Inserting Eq. (5) into Eq. (6) gives

$$G = \frac{k_{\text{AFM}}}{A'} \frac{\left(\frac{V_1^{\circ}V_0}{V_0^{\circ}V_1} \cos \varphi - 1\right) + i \frac{V_1^{\circ}V_0}{V_0^{\circ}V_1} \sin \varphi}{\left(\frac{V_1^{\circ}V_0}{V_0^{\circ}V_1} \cos \varphi - 1\right)^2 + \left(\frac{V_1^{\circ}V_0}{V_0^{\circ}V_1}\right)^2 \sin^2 \varphi} \quad (7)$$

where  $A'$  is an unknown real constant with dimensions of length.

Note that when the displacement becomes large enough to change the contact area, motion will only occur during part of the cycle leading to a sharp rise in harmonic content and a change in the calculated value of  $k_{\text{sample}}$ . We monitor the results to make sure that we are not operating at large enough displacements to produce these effects. We also work with very adhesive surfaces. This leads to substantial penetration of the sphere into the material. Existing theories for adhesive contact are not accurate when the contact radius is comparable to  $R$ , but the contact area is less likely to oscillate in this limit.

In some of the following measurements, we use bulk measurements of  $G$  to determine  $k_{\text{AFM}}/A'$  at one frequency. As will be shown, the AFM and bulk results for  $G'$  and  $G''$  then track over the full range of measured frequencies. When bulk information is not available, one can still obtain useful information about the dimensionless quantity  $\tan \delta$ , which is the ratio of the out-of-phase (imaginary) component to the in-phase (real) component. Because  $k_{\text{AFM}}/A'$  is real,  $\tan \delta$  is given by:

$$\tan \delta = \frac{\text{Imaginary}(k_{\text{sample}})}{\text{Real}(k_{\text{sample}})} = \frac{\text{Imaginary}(G)}{\text{Real}(G)} \quad (8)$$

Inserting Eq. (7) into Eq. (8) gives:

$$\tan \delta = \sin \varphi / [\cos \varphi - (V_0^{\circ}V_1/V_1^{\circ}V_0)] \quad (9)$$

The extra term  $V_0^{\circ}V_1/V_1^{\circ}V_0$  occurs due to the coupling between the spring and the sample. All of the parameters in Eq. (9) ( $\varphi = \theta - \theta_0$ ,  $V_0$ ,  $V_1^{\circ}$ ,  $V_1$ ,  $V_0^{\circ}$ ) are measured in the experiment. Hence,  $\tan \delta$  can directly be calculated and compared to bulk measurements. Additional analyses of force modulation can be found in the literature.<sup>30,36,37</sup>

#### IV. RESULTS AND ANALYSIS

Figure 3 shows the measured amplitude of the atomic force microscope cantilever resting on the oscillating silicon surface (circles) and the adhesive surface (triangles). The modulation amplitude of the atomic force microscope cantilever on the stiff silicon surface is relatively independent of frequency. The modulation amplitude of

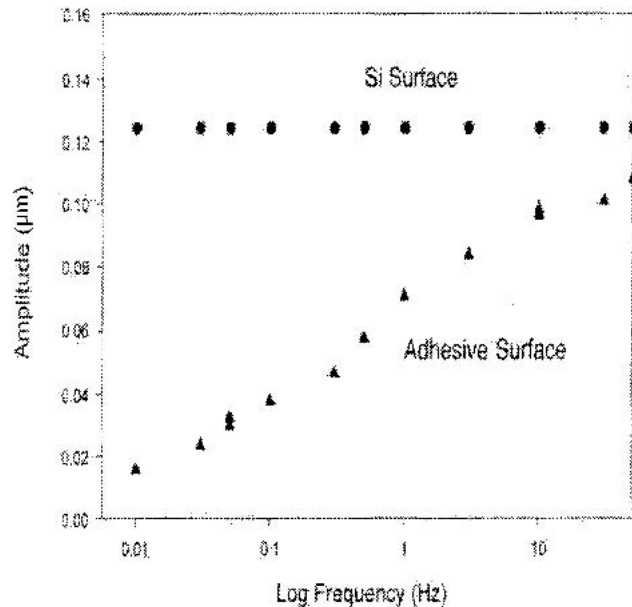


FIG. 3. Measured amplitude of the atomic force microscope cantilever resting on the oscillating Si surface (circles) and the adhesive surface (triangles). The amplitude of oscillation is measured to  $\pm 2\%$  for frequencies above 0.05 Hz and to  $\pm 5\%$  for frequencies below 0.05 Hz.

the atomic force microscope cantilever on the adhesive surface increases with frequency. At low frequency ( $\omega = 0.01$  Hz), the cantilever amplitude was only 13% of the drive amplitude. However, by 10 Hz, the cantilever amplitude was 79% of the drive amplitude. Physically, this means that the polymeric film appeared stiffer as the frequency of oscillations increased, as expected for this polymeric film. In general, the faster a viscoelastic material is deformed, the stiffer it behaves and the less able it is to dissipate energy.

An oscilloscope was used to view the input and photodiode signals. The signals showed normal sine wave behavior indicating the probe remained on the surface during the measurement. In fact, the probe was partially embedded in the adhesive. If the cantilever was disengaged from the adhesive sample, the probe remained in the sample and the cantilever broke. On one occasion, the cantilever did not break when the tip was disengaged. In that case, a large hole, roughly 20  $\mu\text{m}$  diameter, was present on the sample. Thus, it appears that approximately  $15\% \pm 10\%$  of the volume of the sphere was embedded in the sample during the measurement.

Because we could not measure a full load-unload curve of this adhesive sample without breaking the tip, it is impossible to measure the force on the probe. We brought the atomic force microscope probe into contact with the sample under zero load. The atomic force microscope probe became partially embedded in the polymer as evidenced by the initial increasing dc offset. The cantilever deflection was adjusted manually until a stable photodiode reading was maintained.

Figure 4 shows the measured phase  $\theta$  of the atomic force microscope cantilever resting on the oscillating silicon surface (circles) and the adhesive surface (triangles).  $\theta$  is measured relative to the input signal of the function generator. As discussed above, there is a finite phase  $\theta_0$  on the stiff silicon surface due to the phase shift in the PZT and the electronics. It is quite reproducible from sample to sample and tip to tip. For frequencies below 10 Hz,  $\theta_0$  is relatively constant ( $\theta_0 \approx 16^\circ$ ) but it decreases at higher frequencies.

The measured phase of the atomic force microscope cantilever on the adhesive sample  $\theta$  is larger than  $\theta_0$  and varies from  $41^\circ \pm 1^\circ$  to  $28.2^\circ \pm 0.2^\circ$  as the frequency increases from 0.01 Hz to 10 Hz, respectively. Measurements below 0.03 Hz have a larger uncertainty due to the longer time needed to reach equilibrium. The true phase shift  $\varphi$  of the cantilever relative to the PZT displacement is given as  $\varphi = \theta - \theta_0$ . The values of  $\varphi$  decrease from  $22^\circ \pm 1^\circ$  to  $12.2^\circ \pm 0.2^\circ$  as the frequency increases from 0.01 Hz to 10 Hz, respectively.

Using Eq. (9), the  $\tan \delta$  values for the polymer film can be calculated from  $\varphi$  and the ratio of the amplitudes in Fig. 3. Figure 5 compares values of  $\tan \delta$  of the polymer film measured by RDA (circles) and AFM (triangles). For frequencies between 0.01 and 10 Hz, the two techniques measured the same frequency dependence of  $\tan \delta$ . The value of  $\tan \delta$  varies from  $0.47 \pm 0.03$  to  $1.1 \pm 0.16$  as the frequency increases from 0.01 Hz to 10 Hz, respectively. At higher frequencies, the value of  $\varphi$  becomes small, and the error in  $\tan \delta$  becomes large.

In the experimental section of this paper, we noted that the atomic force microscope was linear from monitoring

the 1F, 2F, and 3F components of the photodiode signal. The value of  $\theta_0$  was also found to be independent of the amplitude. These results demonstrate that the atomic force microscope behaves linearly, at least for the amplitudes used in this experiment. To show that the polymer itself exhibited linear viscoelastic behavior, the response of the atomic force microscope cantilever on the polymer was measured at three different amplitudes. The amplitude and phase results are shown in Figs. 6 and 7.

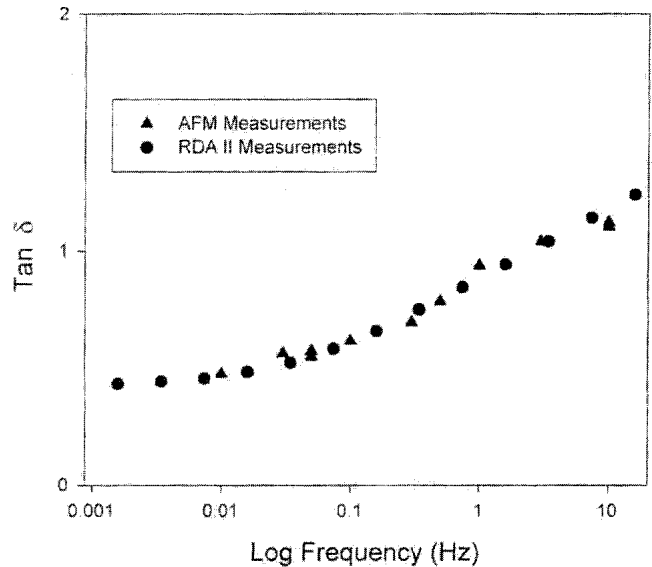


FIG. 5.  $\tan \delta$  measurements of the adhesive film. The triangles represent data taken by the atomic force microscope and calculated according to Eq. (9). The circles represent data on a bulk film 20 times thicker measured by a dynamic shear rheometer (RDA II). For the AFM measurements,  $\tan \delta$  is measured to  $\pm 15\%$ .

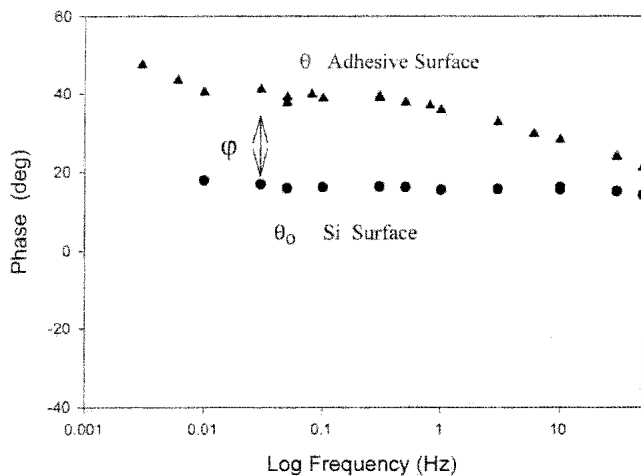


FIG. 4. Measured phase  $\theta$  of the atomic force microscope cantilever resting on the Si surface (circles) and the adhesive surface (triangles). Note that the phase measured on the Si surface is due to the electronics and is not due to the Si surface. The difference between the two measured values of the phase gives the phase  $\varphi$  due to the polymer film (i.e.,  $\varphi = \theta - \theta_0$ ). The phase is measured to  $\pm 0.5^\circ$  for frequencies above 0.05 Hz and to  $\pm 1^\circ$  for frequencies below 0.05 Hz.

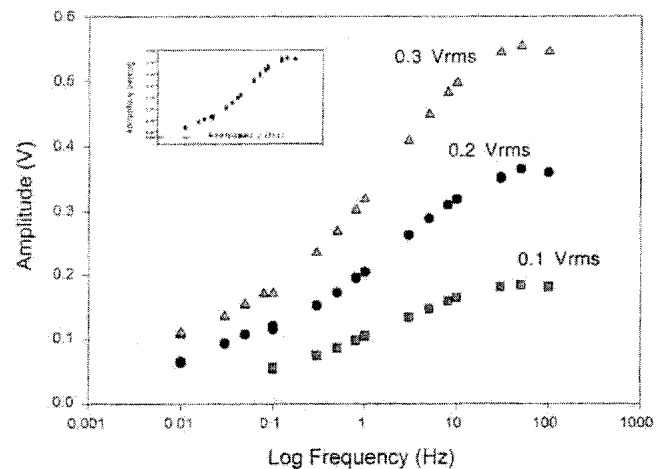


FIG. 6. Measured amplitude of the atomic force microscope cantilever resting on the oscillating adhesive surface as a function of frequency. The amplitudes of the PZT varied with input voltage according to  $dh/dV = (0.579 \mu\text{m} \pm 0.03 \mu\text{m})/V_{\text{rms}}$ . The triangles, circles, and squares represent input voltages of  $0.3 V_{\text{rms}}$ ,  $0.2 V_{\text{rms}}$ , and  $0.1 V_{\text{rms}}$ , respectively. The inset shows the response scaled to  $0.2 V_{\text{rms}}$ . The amplitude of oscillation is measured to  $\pm 2\%$  for frequencies above 0.05 Hz and to  $\pm 5\%$  for frequencies below 0.05 Hz.

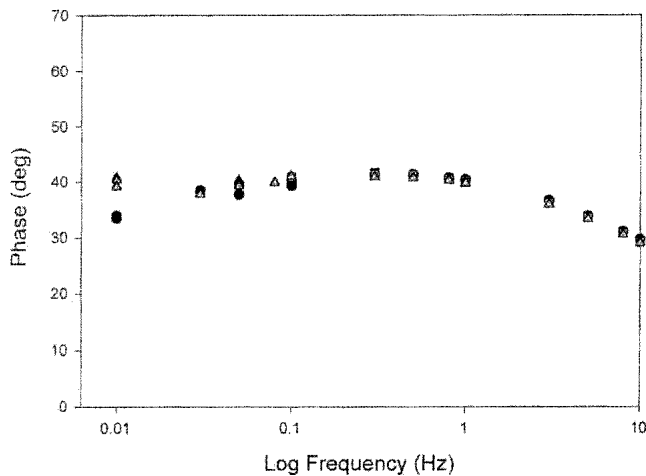


FIG. 7. Measured phase of the atomic force microscope cantilever resting on the oscillating adhesive surface as a function of frequency. The amplitudes of the PZT varied with input voltage according to  $dh/dV = (0.579 \mu\text{m} \pm 0.03 \mu\text{m})/V_{\text{rms}}$ . The triangles, circles, and squares represent input voltages of  $0.3 V_{\text{rms}}$ ,  $0.2 V_{\text{rms}}$ , and  $0.1 V_{\text{rms}}$ , respectively. The phase is measured to  $\pm 0.5^\circ$  for frequencies above 0.05 Hz and to  $\pm 1^\circ$  for frequencies below 0.05 Hz.

The inset in Fig. 6 shows the amplitude scaled to  $0.2 V_{\text{rms}}$  input voltage. The amplitudes of the PZT correspond to  $(0.579 \mu\text{m} \pm 0.03 \mu\text{m})/V_{\text{rms}}$ . The measured phase is independent of the drive amplitude while the amplitude response is linear with the drive amplitude. Hence, linear viscoelastic behavior can be assumed to a first approximation.

## V. DISCUSSION

The results show that the atomic force microscope can easily be modified to give a quantitative measure of the rheological properties of thin polymeric films. For this experiment, a small glass sphere replaced the standard atomic force microscope tip to give a larger contact dimension, and the sample was oscillated at small modulation amplitudes (58 nm to 174 nm) relative to the contact size (about 20  $\mu\text{m}$ ). The results show excellent quantitative agreement between atomic force microscope measurements and bulk measurements, at least for frequencies between 0.01 Hz and 10 Hz.

We have shown that the assumptions of linear behavior of the atomic force microscope and of the polymer film still apply for these conditions. Previous experiments have also shown linear behavior on a styrene-butadiene film, and this linearity is obeyed for amplitudes less than the penetration depth of the tip.<sup>21</sup> The experiments reported here have a penetration depth around 4  $\mu\text{m}$  and amplitudes less than 0.2  $\mu\text{m}$ . Hence, linear behavior is expected, as was the case. In addition, the maximum strain on the polymer sample for the AFM experiments can be estimated by assuming that the dynamics occur on the length scale of the contact diameter, thus,  $\epsilon_{\text{max}} = 0.2 \mu\text{m}/20 \mu\text{m} = 0.01$ . In reality, the

dynamics may occur over a larger length scale, giving rise to a smaller strain. Hence, the strain is less than 1%, which is much less than the 5% and 10% strain measured in the macroscopic experiments where linear viscoelastic behavior was observed.

The equations used to calculate the mechanical properties assume a constant contact area. If the ball is embedded in the sample by 15%, then even if the contact is Hertzian, the change in the contact area for small oscillation amplitude (0.2  $\mu\text{m}$ ) amounts to no more than 4%. With the large adhesion of this adhesive sample, the change in the contact area should be even less. Macroscopic measurements have also shown that small amplitude displacements can give only small changes in the contact diameter.<sup>38</sup>

A number of experimental variables could also affect the measurements. The atomic force microscope cantilever contacts the surface of a material at an angle, generally believed to be around  $11^\circ$  at zero load. Hence, the force on the cantilever is not entirely perpendicular to the surface. If the lower surface moves up and down, then the tip may slip on the sample.<sup>30,39</sup> At frequencies above 10 Hz, the value of  $\varphi$  becomes small and the error in  $\tan \delta$  becomes large. Also, transverse waves may form in the sample due to oscillations that could complicate the forces. Further studies at frequencies above 10 Hz are needed to determine the reliability of the measurements.

Note that Eq. (9) gives the  $\tan \delta$  value in terms of the measurable parameters  $\varphi$ ,  $V_0$ ,  $V_1^\circ$ ,  $V_1$ , and  $V_0^\circ$ . Determination of the spring constant is not required nor is knowledge of the contact dimension necessary. If the exact value of the modulus is desired, then the spring constant, contact dimensions, and an accurate model are required. Equation (7) lumps all the unknowns together in one geometric prefactor  $k_{\text{AFM}}/A'$ . If  $k_{\text{AFM}}/A'$  can be considered constant, then  $G'$ , as given by the real part of Eq. (7), should at least be proportional to  $G'$  measured by the RDA. Figure 8 shows  $G'$  measured by the RDA and  $G'$  calculated by the real part of Eq. (7), assuming  $k_{\text{AFM}}/A' = 7 \times 10^4 \text{ N/m}^2$ . There is good overlap between the two measurements, indicating that it is reasonable to consider the geometric prefactor as a constant. A similar agreement was found for  $G''$  (Imaginary  $G$ ) again using  $k_{\text{AFM}}/A' = 7 \times 10^4 \text{ N/m}^2$ . The exact mathematical form of  $k_{\text{AFM}}/A'$ , especially for viscoelastic solids and small contacts, has currently not been fully evaluated for these experimental conditions. In the nonadhesive (Hertzian) limit,  $k_{\text{AFM}}/A'$  is given by  $k_{\text{AFM}}/8a \approx 6 \times 10^5 \text{ N/m}^2$ , which is about 10 times higher than found empirically.<sup>34</sup> A more thorough understanding of the contact mechanics of nanometer contacts of viscoelastic materials is required to determine the significance of this discrepancy.

The adhesive film measured by the RDA was 20 times thicker than that measured by AFM. The estimated contact diameter is comparable to the film thickness. As a

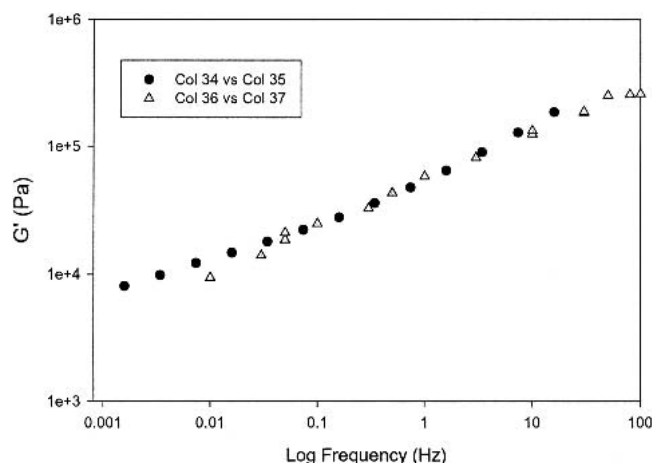


FIG. 8. Measurements of  $G'$  [given as the real part of Eq. (7)] assuming  $k_{AFM}/A' = 7 \times 10^4 \text{ N/m}^2$ . The AFM measurements are shown as triangles whereas the circles represent data measured on the RDA.  $G'$  is measured to  $\pm 10\%$ .

general rule, the underlying substrate influences the measurement at approximately 3 times the contact diameter or less than 10 times the indentation depth.<sup>40</sup> Because the adhesive was approximately twice as thick as three times the contact diameter, the measurements should not be affected by the underlying substrate. In addition, the amplitude of oscillation (58 nm to 174 nm) and the indentation depth (approximately 4  $\mu\text{m}$ ) was much smaller than the film thickness (130  $\mu\text{m}$ ), supporting the conclusion that the measurements mainly reflect the adhesive properties. Future experiments will investigate thinner films to determine the limits of the measurement and investigate how the substrate may influence the mechanical properties.

As previously mentioned, the sample must be deformed if AFM is to be used to measure the mechanical properties. For this to occur, the indenter spring stiffness must be comparable to the contact stiffness. Unfortunately, a limited number of cantilever spring constants are commercially available. For mechanical properties of stiffer films to be measured, stiffer cantilevers are necessary. Measurements on stiffer films will give rise to a smaller contact dimension, and this may lead to an error in the assumption of constant contact area. The roughness of the probe may also become important, which is not the case for softer materials. Future measurements will address these issues.

The results presented here sample the bulk rheological properties because the contact radius is much larger than the characteristic length scales. By varying the sphere radius or tip geometry, the contact radius can change from nanometer to micrometer dimensions, allowing for a wide range of contact sizes. This will allow measurements over the range of length scales important in polymer science, such as the radius of gyration.

Mechanical property measurements by AFM seem particularly well suited to measure biological materials such as cells and vesicles. The AFM offers the spatial resolution required to measure such small samples, and the relatively weak spring constant allows the small forces to be measured. Furthermore, the method will allow for measurements in various environments.

## VI. CONCLUSIONS

The mechanical properties of a commercial pressure-sensitive adhesive transfer tape were measured by AFM. Both oscillation amplitude and phase of an atomic force microscope cantilever resting on an oscillating polymer surface were recorded as a function of frequency (0.01 Hz to 10 Hz). The value of  $\tan \delta$  varied from  $0.47 \pm 0.03$  to  $1.1 \pm 0.16$  as the frequency increased from 0.01 Hz to 10 Hz, respectively. The atomic force microscope measurement gave the same frequency dependence of  $\tan \delta$  as that measured by macroscopic techniques. The results demonstrate that the AFM technique can quantitatively measure rheological properties of thin polymeric films.

## ACKNOWLEDGMENTS

This paper represents an official contribution of the National Institute of Standards and Technology; not subject to copyright in the United States. P.M.M. would like to thank the NIST ATP Program for partially supporting this work. We would also like to thank Mark Robbins and Grady White for helpful suggestions. (Disclaimer: Certain commercial equipment, instruments, or materials are identified in this paper to adequately specify the experimental procedure. Such identification does not imply recommendation or endorsement by the National Institute of Standards and Technology nor does it imply that the materials or equipment are necessarily the best available for the purpose.)

## REFERENCES

1. B. Bhushan, J.N. Israelachvili, and U. Landman, *Nature* **374**, 607 (1995).
2. G.M. Pharr and W.C. Oliver, *MRS Bull.* **17**, 28 (1992).
3. J.B. Pethica, R. Hutchings, and W.C. Oliver, *Philos. Mag. A*, **48**, 593 (1983).
4. H.M. Pollock, *ASM Handbook*, (ASM International, Materials Park, OH, 1992), pp. 419–429.
5. J.L. Loubet, W.C. Oliver, and B.N. Lucas, *J. Mater. Res.* **15**, 1195 (2000).
6. S.A.S. Asif, K.J. Wahl, and R.J. Colton, *Rev. Sci. Instrum.* **70**, 2408 (1999).
7. B.J. Briscoe, L. Fiori, and E. Pelillo, *J. Phys. D.:Appl. Phys.* **31**, 2395 (1998).
8. S.M. Hues, C.F. Draper, and R.J. Colton, *J. Vac. Sci. Technol. B* **12**, 2211 (1994).

9. N.A. Burnham and R.J. Colton, *J. Vac. Sci. Technol. A* **7**, 2906 (1989).
10. G. Gillies, C.A. Prestidge, and P. Attard, *Langmuir* **18**, 1674 (2002).
11. C. Reynaud, F. Sommer, C. Quet, N. El Bounia, and T.M. Duc, *Surf. Interface Anal.* **30**, 185 (2000).
12. J.D. Ferry, *Viscoelastic Properties of Polymers*, 3rd ed. (John Wiley, New York, 1980).
13. C.W. Macosko, *Rheology Principles, Measurements, and Applications* (Wiley-VCH, New York, 1994).
14. E. Barthel and G. Haiat, *Langmuir* **18**, 9362 (2002).
15. T. Ting, *J. Appl. Mech.* **35**, 248 (1968).
16. T. Ting, *J. Appl. Mech.* **33**, 845 (1966).
17. M. Giri, D. Bousfield, and W.N. Unertl, *Tribol. Lett.* **9**, 33 (2000).
18. C.Y. Hui, J.M. Baney, and E.J. Kramer, *Langmuir* **14**, 6570 (1998).
19. T. Kajiyama, K. Tanaka, I. Ohki, S.R. Ge, J.S. Yoon, and A. Takahara, *Macromolecules* **27**, 7932 (1994).
20. M.C. Friedenbergs and C.M. Mate, *Langmuir* **12**, 6138 (1996).
21. C. Fretigny, C. Basire, and V. Granier, *J. Appl. Phys.* **82**, 43 (1997).
22. A. Paiva, N. Sheller, M.D. Foster, A.J. Crosby, and K.R. Shull, *Macromolecules* **33**, 1878 (2000).
23. X.P. Wang, X.D. Xiao, and O.K.C. Tsui, *Macromolecules* **34**, 4180 (2001).
24. M. Giri, D.B. Bousfield, and W.N. Unertl, *Langmuir* **17**, 2973 (2001).
25. Y. Pu, S.R. Ge, M. Rafailovich, J. Sokolov, Y. Duan, E. Pearce, V. Zaitsev, and S. Schwarz, *Langmuir* **17**, 5865 (2001).
26. R.E. Mahaffy, C.K. Shih, F.C. MacKintosh, and J. Kas, *Phys. Rev. Lett.* **85**, 880 (2000).
27. R.W. Carpick, D.F. Ogletree, and M. Salmeron, *Appl. Phys. Lett.* **70**, 1548 (1997).
28. K.J. Wahl, S.V. Stepanowski, and W.N. Unertl, *Tribol. Lett.* **5**, 103 (1998).
29. K. Tanaka, A. Taura, S.R. Ge, A. Takahara, and T. Kajiyama, *Macromolecules* **29**, 3040 (1996).
30. P.E. Mazeran and J.L. Loubet, *Tribol. Lett.* **7**, 199 (1999).
31. D.J. Yarusso, *J. Adhes.* **70**, 299 (1999).
32. A.V. Pocius, *Adhesion and Adhesives Technology* (Hanser Publishers, Munchen, Germany, 1997).
33. W.A. Ducker, T.J. Senden, and R.M. Pashley, *Nature* **353**, 239 (1991).
34. K.L. Johnson, *Contact Mechanics* (Cambridge University Press, Cambridge, U.K., 1985).
35. G.Y. Choi, S.J. Kim, and A. Ulman, *Langmuir* **13**, 6333 (1997).
36. N.A. Burnham, G. Gremaud, A.J. Kulik, P.J. Gallo, and F. Oulevey, *J. Vac. Sci. & Technol. B* **14**, 1308 (1996).
37. M. Radmacher, R.W. Tilmann, and H.E. Gaub, *Biophys. J.* **64**, 735 (1993).
38. A.R. Savkoor and G.A.D. Briggs, *Proc. R. Soc. (London) Ser. A* **356**, 103 (1977).
39. R.J. Warmack, X.Y. Zheng, T. Thundat, and D.P. Allison, *Rev. Sci. Instrum.* **65**, 394 (1994).
40. G.M. Pharr, W.C. Oliver, and F.R. Brotzen, *J. Mater. Res.* **7**, 613 (1992).